Selective inhibition of plasma membrane calcium ATPase 4 improves angiogenesis and vascular reperfusion

Sathishkumar Kurusamy[1], Dolores López-Maderuelo[2,3], Robert Little[4], David Cadagan[1], Aaron M Savage[5], Jude C Ihugba[1], Rhiannon R Baggott[1], Farjana B Rowther[6], Sara Martínez-Martínez[2], Pablo Gómez-del Arco[2,3,7], Clare Murcott[1], Weiguang Wang[8], J Francisco Nistal[9], Delvac Oceandy[4], Ludwig Neyses[4,10], Robert N Wilkinson[5], Elizabeth J Cartwright[4], Juan Miguel Redondo[2,3,*], Angel Luis Armesilla[1,*]

[1]Cardiovascular Molecular Pharmacology Laboratory, School of Pharmacy, [6]Brain Tumor UK Neuro-oncology Research Centre, and [8]Oncology Laboratory, Research Institute in Healthcare Science, Faculty of Science and Engineering, University of Wolverhampton, Wolverhampton, UK; [2]Gene Regulation in Cardiovascular Remodelling and Inflammation Group, Centro Nacional de Investigaciones Cardiovasculares, Madrid, Spain; [3]CIBERCV; [4]Division of Cardiovascular Sciences, University of Manchester, Manchester Academic Health Sciences Centre, Manchester, UK; [5]Department of Infection, Immunity & Cardiovascular Disease & Bateson Centre, University of Sheffield, UK; [7]Department of Molecular Biology, Universidad Autonoma de Madrid (C.B.M.-S.O.), Madrid, Spain; [9]Cardiovascular Surgery, Hospital Universitario Marqués de Valdecilla, IDIVAL, Facultad de Medicina, Universidad de Cantabria, Santander, Spain; [10]University of Luxembourg.

*__Correspondence:__
Juan Miguel Redondo, Gene Regulation in Cardiovascular Remodelling and Inflammation Group, Centro Nacional de Investigaciones Cardiovasculares, Melchor Fernandez Almagro 3, E-28029, Madrid, Spain, e-mail: jmredondo@cnic.es
Or
Angel Luis Armesilla, Cardiovascular Molecular Pharmacology Laboratory, Research Institute in Healthcare Science, School of Pharmacy, Faculty of Science and Engineering, University of Wolverhampton, Wulfruna Street, Wolverhampton, WV1 1SB, UK, e-mail: A.Armesilla@wlv.ac.uk

Number of words: 8,417

Abstract

Aims: Ischaemic cardiovascular disease is a major cause of morbidity and mortality worldwide. Despite promising results from pre-clinical animal models, VEGF-based strategies for therapeutic angiogenesis have yet to achieve successful reperfusion of ischaemic tissues in patients. Failure to restore efficient VEGF activity in the ischaemic organ remains a major problem in current pro-angiogenic therapeutic approaches. Plasma membrane calcium ATPase 4 (PMCA4) negatively regulates VEGF-activated angiogenesis via inhibition of the calcineurin/NFAT signalling pathway. PMCA4 activity is inhibited by the small molecule aurintricarboxylic acid (ATA). We hypothesise that inhibition of PMCA4 with ATA might enhance VEGF-induced angiogenesis.

Methods and Results: We show that inhibition of PMCA4 with ATA in endothelial cells triggers a marked increase in VEGF-activated calcineurin/NFAT signalling that translates into a strong increase in endothelial cell motility and blood vessel formation. ATA enhances VEGF-induced calcineurin signalling by disrupting the interaction between PMCA4 and calcineurin at the endothelial-cell membrane. ATA concentrations at the nanomolar range, that efficiently inhibit PMCA4, had no deleterious effect on endothelial-cell viability or zebrafish embryonic development. However, high ATA concentrations at the micromolar level impaired endothelial cell viability and tubular morphogenesis, and were associated with toxicity in zebrafish embryos. In mice undergoing experimentally-induced hindlimb ischaemia, ATA treatment significantly increased the reperfusion of post-ischaemic limbs.

Conclusions: Our study provides evidence for the therapeutic potential of targeting PMCA4 to improve VEGF-based pro-angiogenic interventions. This goal will require the development of refined, highly selective versions of ATA, or the identification of novel PMCA4 inhibitors.

Keywords: PMCA4, angiogenesis, ATA, calcineurin/NFAT, VEGF

1. Introduction

Ischaemic cardiovascular diseases (including ischaemic heart disease, peripheral arterial disease, and stroke) constitute a leading cause of morbidity and mortality worldwide [1]. In some patients, bypass surgery and interventional endovascular procedures can successfully restore blood flow to the ischaemic tissue [2,3]. However, the distribution and diffuseness of arterial occlusions preclude surgical revascularization in a high proportion of patients [3]. Therapeutic strategies to promote the formation of new blood vessels in the ischaemic organ (referred to as therapeutic angiogenesis) constitute a promising alternative for these patients [3-5].

Angiogenesis, the formation of new blood vessels from pre-existing ones, is a tightly regulated process involving the participation of several pro- and anti-angiogenic factors [6]. One of the critical pro-angiogenic factors is vascular endothelial growth factor (VEGF) [7]. A number of gene-based and protein-based approaches have been developed to deliver exogenous VEGF to ischaemic tissues [5]. Data obtained in animal models of myocardial and limb ischaemic disease demonstrated that VEGF-based pro-angiogenic therapies induce successful reperfusion of the ischaemic organ [8]. Unfortunately, to date clinical translation of these procedures has produced only limited patient benefit [9]. The reasons for the lack of clinical success with therapeutic angiogenesis approaches are complex, but one central problem in current approaches is failure to restore efficient VEGF activity in the ischaemic organ [5,8,9]. Design of new, more effective treatments requires a deep understanding of the molecular and biochemical processes governing VEGF-induced angiogenesis.

We recently reported a novel role for plasma membrane calcium ATPase 4 (PMCA4) as a negative regulator of VEGF-activated angiogenesis [10]. PMCAs are enzymatic high-affinity systems that export calcium from the cytosol to the extracellular environment [11]. There are four PMCA isoforms (PMCA1-4) encoded by four distinct genes [11]. PMCA1 and 4 are expressed ubiquitously, whereas PMCA2 and 3 are restricted to highly specialised cells and tissues [11]. PMCA4 is the major isoform present in endothelial cells [12]. Our previous work showed that PMCA4 attenuates VEGF-induced angiogenesis by establishing an inhibitory

interaction with the signalling protein calcineurin [10]. Calcineurin is a serine/threonine phosphatase activated by increases in cytosolic calcium concentration [13]. Activated calcineurin mediates dephosphorylation of NFAT (nuclear factor of activated T cells) transcription factors, promoting their translocation to the nucleus and the subsequent expression of NFAT-target genes [14]. The calcineurin/NFAT signalling axis plays a critical role in VEGF-induced angiogenesis [15,16]. PMCA4 is thought to downregulate calcineurin activity by tethering it to low-calcium micro-domains created by the pump's calcium expulsion action and, in so doing, impair VEGF-activated pro-angiogenic signalling [10]. We therefore hypothesize that pharmacological blockade of PMCA4 function, and thus suppression of the negative effect of PMCA4 on angiogenesis, might potentiate the efficiency of therapeutic strategies involving VEGF. Supporting this possibility, we previously reported more efficient limb reperfusion in *PMCA4*$^{-/-}$ knockout mice undergoing femoral artery ligation than in their wild-type littermates [10].

A recent study showed that low concentrations of the small molecule aurintricarboxylic acid (ATA) strongly inhibit the calcium extrusion activity of PMCA4 without affecting the activity of PMCA1 or other major calcium pumps such as SERCA and the Na^+/K^+ ATPase [17]. This finding prompted us to examine whether inhibition of PMCA4 with ATA enhances VEGF-induced angiogenesis.

Here, we show that treatment of primary endothelial cells with low concentrations of ATA results in a remarkable increase in VEGF-mediated activation of the calcineurin/NFAT pathway and in the expression of the VEGF-induced, NFAT-dependent, pro-angiogenic protein RCAN1.4. Inhibition of PMCA4 with ATA also enhances endothelial cell motility and tubular morphogenesis, with no harmful effects on the cells. These results highlight the clinical potential of targeting PMCA4 to improve VEGF-based therapeutic interventions that promote blood vessel formation in patients suffering from ischaemic cardiovascular disease.

2. Materials and methods

2.1. Cells and Cell Culture

Human umbilical vein endothelial cells (HUVEC) were purchased from TCS Cellworks and cultured in tissue culture flasks pre-coated with 0.1% gelatin in endothelial cell growth medium (ECGM, PromoCell) supplemented with ECGM-supplement mix and 1% penicillin/streptomycin/amphotericin B (Sigma-Aldrich). HUVECs were used at passages 6-8.

Mouse lung endothelial cells (MLEC) were purified from wild-type or PMCA4-null mice as described [10]. Generation and characterization of PMCA4 knockout mice has been previously reported [18].

2.2. Luciferase reporter assay

HUVECs were infected with Ad-NFAT-Luc (a replication-deficient adenovirus harbouring an NFAT-dependent, luciferase-based reporter system) at a multiplicity of infection (MOI) of 50. Generation of Ad-NFAT-Luc-infected particles was as described [10]. Infected cells were incubated in ECGM containing 0.5% fetal calf serum for 16 hours and then stimulated with VEGF (25 ng/ml) for 6 hours. Luciferase activity was determined as described [19].

2.3. siRNA gene knock-down

siRNA-mediated knock-down of *PMCA4* gene expression was performed using “ON-TARGET-plus SMART pool human ATP2B4” (Thermo Scientific). “ON-TARGET-plus non-targeting pool control duplexes” (Thermo Scientific) was used as a control.

For siRNA transfection, HUVECs were plated in 0.1% gelatin pre-coated 6-well tissue culture plates (3 x 10^5 cells/well) and incubated overnight. The following morning, cells were washed with PBS and incubated in serum-free, antibiotic-free OPTIMEM medium for 1 hour. Then, 100 pmol of siRNA/well were transfected using 5 µl of Lipofectamine 2000 (Thermo Scientific). Transfection medium was removed after incubation for 6 hours, and substituted by ECGM supplemented with ECGM-supplement mix and 1% penicillin/streptomycin/amphotericin B (Sigma-Aldrich). Cells were incubated for 72 hours and then used for further experiments.

Quantitative Real-Time PCR

Total RNA from HUVECs was extracted using the "Total RNA purification kit" (Norgen) and cDNA synthesis was performed with 0.5 µg of total RNA using the "High capacity cDNA reverse transcription kit" (Applied Biosystems). *PMCA4* RNA expression was determined by qRT-PCR using TaqMan Gene Expression Assay (Hs00608066_m1) in a 7500 Fast Real-Time PCR System (Applied Biosystems, UK). PCR cycling conditions consisted of an initial enzyme activation step at 95°C for 10 minutes, followed by denaturation at 95°C for 15 seconds, and annealing and extension at 60°C for 1 minute for 40 cycles. Ct value was normalized using the Ct values for the housekeeping gene *Hprt-1* (TaqMan Gene Expression Assay, Hs99999909_m1). Analysis of data was carried out using the comparative $2^{-\Delta\Delta CT}$ method.

2.4. Western Blot

Total proteins were isolated by direct lysis of HUVECs, treated as indicated, in NuPAGE LDS sample buffer containing 0.05% β-mercaptoethanol. Membrane-associated proteins were isolated using the ProteoExtract Subcellular Proteome Extraction Kit (Calbiochem) as reported [20].

We have noticed that repeated and prolonged boiling degrades endothelial PMCA4; therefore we minimised repeated cycles of freeze-thawing-boiling. Protein samples were boiled for 1 minute and then resolved by SDS-PAGE as described [21]. Antibody sources and conditions are described in detail in the online Supplementary Material.

2.5. Immunoprecipitation

HUVECs were stimulated for 4 hours with VEGF (25 ng/ml) in the presence of ATA (250 nM) or vehicle (DMSO), and PMCA4/calcineurin complexes were immunoprecipitated from 4 mg total protein extract with anti-calcineurin A monoclonal antibody (Sigma) using the Pierce Co-Immunoprecipitation Kit. To immunoprecipitate the PMCA4/eNOS complex, the same conditions were used except that cells were treated for only 5 minutes and protein lysates were incubated with anti-PMCA 5F10 monoclonal antibody.

Levels of PMCA4, calcineurin, or eNOS in the immunoprecipitates were determined by western blot using anti-PMCA4 (JA3), anti-calcineurin A, or anti-eNOS antibodies.

2.6. Wound healing migration assay

Cell migration of HUVECs and MLECs, treated as indicated, was assayed using the Cytoselect™ 24-well Wound Healing Assay kit (Cell Biolabs). Images were captured with a Nikon DSFi1 digital camera coupled to a Nikon ECLIPSE TS100 microscope at 4x magnification. Cell-free area was quantified with ImageJ software.

2.7. Matrigel tube-formation assay

HUVECs were plated onto Geltrex Reduced Growth-Factor Matrix (Invitrogen) in Medium 200 with no phenol red and supplemented with 2% fetal calf serum and 50 ng/ml growth factor (VEGF or bFGF) in the presence of ATA at the indicated concentration or DMSO as a control. Tube formation was quantified after incubation at 37°C for 16 hours. Images were recorded with a Nikon DSFi1 digital camera coupled to a Nikon ECLIPSE TS100 microscope at 4x magnification.

2.8. MTT assay

HUVECs were seeded on 96-well tissue culture plates (without gelatin pre-coating) at a density of 2.5 x 10^4 cells/well in supplemented ECGM (PromoCell). Cell viability was determined by MTT assay [22] the morning after cell plating (Time=0) and then after 3 and 6 days of incubation in supplemented ECGM containing VEGF (25 ng/ml) and ATA at the indicated concentration or DMSO as control.

2.9. Zebrafish embryo viability

Zebrafish embryos *Tg(kdrl:HRAS-mCherry; flk1:EGFP-nls*) [23,24] were manually dechorionated and incubated in increasing concentrations of ATA or DMSO from 30 hours post fertilisation (hpf) for 24 hours. Vascular morphology was imaged at 54 hpf using a Zeiss Lightsheet Z.1 microscope. Experiments were performed under UK Home Office licence 40/3708.

2.10. Murine hindlimb ischaemia

Unilateral hindlimb ischaemia was induced by femoral artery ligation in 12-week-old C57/BL6 mice anaesthetised with 2% isoflurane *via* inhalation. To induce hindlimb ischaemia maintaining minimal blood flow to the limb, we ligated a short fragment of the femoral artery in

proximal and distal positions and excised the intervening segment (this procedure corresponds to the experiments shown in Fig 7). In a separate set of experiments, to totally blunt blood flow to the limb, we performed femoral ligation and excision of the intervening segment but on this occasion we ligated and excised a longer femoral segment to induce deep acute ischaemia (this procedure corresponds to the experiments shown in Fig S5). In all cases, ATA (5 mg/kg) or DMSO (vehicle) was administered intraperitoneally 2 hours after the operation, and then daily as indicated. Blood flow was measured in the sham-operated and ischaemic limbs of anaesthetised animals before surgery, 2 hours after the operation, and at the indicated times using a Laser Doppler Perfusion Imager System (Moor Instruments). Mice were sacrificed in an euthanasia chamber with 70% CO_2.

Mouse studies were approved by Animal Care and Ethics committee at the Centro Nacional de Investigaciones Cardiovasculares and conformed to directive 2010/63EU and recommendation 2007/562/EC regarding the protection of animals used for experimental and other scientific purposes.

2.11. Nitric oxide determination

To determine intracellular nitric oxide bioavailability HUVECs were incubated for 3 hours in basal ECGM (Promocell) containing 0.5% fetal bovine serum (FBS). After serum starvation, L-arginine was added to a 100 µM final concentration and cells were incubated for 15 minutes. Cells were then loaded for 30 minutes with 10 µM of the NO-sensitive fluorescence probe DAF-FM (Molecular Probes). Dye-containing medium was removed and replaced with basal ECGM, 0.5% FBS. Cells were incubated for 45 minutes at 37°C, and then NO synthesis was induced by stimulation for 5 minutes with VEGF (25 ng/ml) in the presence of ATA (250 nM) or vehicle (DMSO). After treatment, cells were washed with PBS and fixed in formalin (Sigma). DAF-FM fluorescence was detected using a ZEISS LSM 880 confocal laser scanning microscope.

2.12. Immunohistochemistry

Tibialis muscle isolated from non-ischaemic (sham-operated) or ischaemic limbs were fixed in 4% formalin solution, then incubated in 30% saccharose solution, embedded in OCT, frozen in

liquid nitrogen, and finally cut on a cryotome. VEGF expression was detected by immunohistochemistry using a 1:750 dilution of an anti-VEGF-A rabbit polyclonal antibody (1 mg/ml, Sigma-Aldrich). A biotinylated anti-rabbit IgG was used as secondary antibody at a 1:500 dilution. Samples were incubated with a 1:500 dilution of HPR-conjugated streptavidin. Substrate staining was developed with diaminobenzidine (DAB; Vector Laboratories).

2.13. Statistical analysis

Results are shown as mean ± S. E. Significance of differences between two groups was analysed by unpaired, two-tailed Student's *t* test. One-way ANOVA with *post hoc* Tukey's comparison test was used for comparison among groups. Differences were considered statistically significant at $P \leq 0.05$.

3. Results

3.1. ATA enhances VEGF-induced calcineurin signalling in endothelial cells by disrupting the PMCA4/calcineurin interaction

Our previous work demonstrated that PMCA4 negatively modulates VEGF-induced activation of the calcineurin/NFAT signal transduction pathway in endothelial cells [10]. The identification of the small molecule ATA as a PMCA4 inhibitor [17] prompted us to investigate whether ATA-mediated PMCA4 inhibition potentiates VEGF-induced calcineurin/NFAT signalling.

To explore this possibility, primary HUVECs were infected with the NFAT-dependent, luciferase-based adenoviral reporter vector Ad-NFAT-Luc. Inhibition of PMCA4 is reached at low ATA concentrations in the range of 250 nM [17]. We therefore used this concentration of ATA in our experiments to achieve inhibition of PMCA4 while avoiding inhibitory effects on other cellular proteins that have been shown to require much higher ATA concentrations to be inhibited. Treatment of Ad-NFAT-Luc-infected HUVECs with 250 nM ATA increased VEGF-induced calcineurin/NFAT pathway activation by 78.1% (Fig 1A).

Further analysis on the functional consequences of boosting calcineurin signalling with ATA showed that VEGF-induced protein expression of the NFAT-dependent gene RCAN1.4 was also significantly enhanced (56.8%) by ATA treatment (Fig 1B).

These data indicate that ATA potentiates the VEGF-induced activation of the calcineurin/NFAT pathway in endothelial cells, and that this effect is translated into enhanced expression of NFAT-target genes such as *RCAN1.4*.

PMCA4 is thought to downregulate calcineurin/NFAT pathway activity through a molecular interaction that sequesters calcineurin into low-calcium micro-domains created by the pump's calcium extrusion activity [25]. Supporting this idea, disruption of the PMCA4/calcineurin interaction notably potentiates calcineurin/NFAT signalling [10]. We therefore next examined whether the ATA-enhanced calcineurin signalling is associated with changes in the interaction between the two proteins. Membrane-associated proteins were isolated from HUVECs treated with VEGF in the presence or absence of ATA and analysed for the content of PMCA4 and calcineurin. ATA treatment significantly reduced the level of membrane-associated calcineurin,

whereas the levels of PMCA4 remain unaffected (Fig 2A), suggesting that treatment of HUVECs with ATA releases calcineurin from its interaction with PMCA4 in the plasma membrane. Analysis of whole-cell extracts revealed similar levels of calcineurin in control (DMSO) and ATA-treated cells, excluding an effect of ATA on calcineurin expression (Fig 2B). Total levels of PMCA4 were similarly unaffected in the same samples (Fig 2B).

To confirm that the decrease in membrane-associated calcineurin was due to disruption of the PMCA4/calcineurin interaction, we performed immunoprecipitation experiments. Protein extracts from HUVECs stimulated with VEGF in the presence or absence of 250 nM ATA were immunoprecipitated with anti-calcineurin antibody. Western blot analysis of the immunoprecipitated proteins revealed that ATA treatment markedly reduced the amount of PMCA4 co-precipitated with calcineurin, suggesting dissociation of the PMCA4/calcineurin complex (Fig 2C). No significant differences were found in the amount of immunoprecipitated calcineurin in control and ATA-treated cells (Fig 2C), excluding an effect of ATA on the affinity of the immunoprecipitating antibody for calcineurin.

Together, these data suggest that treatment of endothelial cells with ATA liberates calcineurin from its interaction with PMCA4, thereby potentiating VEGF-mediated activation of calcineurin/NFAT signalling and the subsequent expression of NFAT-target genes such as *RCAN1.4*.

3.2. ATA increases VEGF-mediated endothelial cell motility and blood vessel formation

PMCA4-mediated inhibition of calcineurin/NFAT signalling negatively regulates endothelial cell migration and tubular morphogenesis [10]. The enhanced calcineurin/NFAT signalling induced by ATA in VEGF-stimulated HUVECs (Fig 1) suggested that ATA might reverse the negative effect of PMCA4 on these angiogenic processes.

In wound-healing migration assays, exposure of VEGF-stimulated HUVECs to ATA increased cell migration by 58.4% (Fig 3A).

To determine whether the ATA-dependent increase in endothelial cell motility involves PMCA4 inhibition, and is not the consequence of off-target effects, migration assays were conducted with mouse lung endothelial cells (MLECs) isolated from *PMCA4*$^{-/-}$ knockout mice or their

wildtype littermates. Consistent with our published observations [10], PMCA4-deficient cells migrated over longer distances than their wildtype counterparts (Fig 3B). However, whereas ATA increased wildtype MLEC migration by 64.7%, it had no effect on the migration of PMCA4-deficient MLECs (Fig 3B).

To investigate whether the ATA-mediated enhanced endothelial cell motility is linked to disruption of the PMCA4/calcineurin interaction, we performed cell migration assays using HUVECs infected with Ad-ID4, an adenoviral vector encoding a PMCA4 region that successfully disrupts association between the two proteins [10]. As a control, HUVECs were infected with an adenovirus encoding β-Galactosidase (Ad-LacZ). ATA increased the migration of Ad-LacZ-infected cells (Fig 3C). As we previously reported [10], disruption of the PMCA4/calcineurin interaction in Ad-ID4-infected HUVECs increased cell migration (Fig 3C), however ATA-treatment did not further increase migration (Fig 3C). Ad-ID4-infected cells treated with DMSO or ATA expressed equal amounts of ID4, excluding an effect of ATA on adenovirus infection efficiency (Fig S1). These data not only confirm the implication of PMCA4 in ATA-enhanced endothelial cell migration, but also reveal that disruption of the interaction between PMCA4 and calcineurin is a key molecular mediator of this process.

PMCA4 and the calcineurin/NFAT pathway both have well-established roles in the regulation of blood vessel formation [10,15,16]. We therefore next investigated the effect of ATA on endothelial cell tubular morphogenesis. Consistent with previous studies [10,16], VEGF increased the ability of HUVECs to form capillary-like structures in Matrigel assays (Fig 4A). VEGF-induced tube formation was further enhanced by co-treatment with ATA (38.9% increase with respect to control cells) (Fig 4A). To substantiate the involvement of PMCA4 on the boost in VEGF-induced endothelial cell tubular morphogenesis exerted by ATA, we suppressed *PMCA4* expression in endothelial cells using siRNA-mediated technology (Fig S2). ATA significantly enhanced endothelial cell tubular morphogenesis in VEGF-stimulated cells transfected with a control non-target siRNA (si-NT) (Fig 4B). As expected, suppression of *PMCA4* expression in cells transfected with siRNA targeting PMCA4 (si-PMCA4) increased the ability of the cells to form capillary-like structures in response to VEGF (Fig 4B), however

ATA failed to further increase tubular morphogenesis in these cells (Fig 4B). This result demonstrates the involvement of PMCA4 in the enhancement of blood vessel formation induced by ATA in endothelial cells stimulated with VEGF.

Interestingly, ATA did not boost tubular morphogenesis in HUVECs stimulated with basic fibroblast growth factor (bFGF), a pro-angiogenic factor that does not activate calcineurin signalling [16] (Fig 4C).

These observations suggest that inhibition of PMCA4 with ATA markedly enhances VEGF-induced endothelial cell motility and tubular morphogenesis in a calcineurin/NFAT-dependent manner.

Altogether, these results highlight the clinical potential of PMCA4 inhibition and/or disruption of the PMCA4/calcineurin interaction to design novel therapeutic approaches that improve VEGF-induced angiogenesis in patients with cardiovascular ischaemic disease.

3.3. ATA promotes PMCA4/eNOS interaction and attenuates nitric oxide synthesis in endothelial cells

Our results in this work establish a major role for the calcineurin/NFAT signalling pathway in the enhancement of VEGF-induced angiogenesis upon inhibition of PMCA4 with ATA; however, they do not exclude the potential participation of other signalling pathways. In addition to calcineurin, we recently showed that PMCA4 also downregulates the activity of eNOS and the subsequent production of nitric oxide (NO) in endothelial cells [26]. The pro-angiogenic properties of NO are well established [27, 28], and VEGF activates eNOS-mediated NO production in endothelial cells [29]. Thus we decided to investigate the effect of ATA on the PMCA4/eNOS interaction, and in the induction of NO synthesis mediated by VEGF in endothelial cells. For this purpose, protein lysates isolated from HUVECs stimulated with VEGF in the presence or absence of 250 nM ATA were immunoprecipitated with the anti-PMCA antibody 5F10. Western blot analysis of immunoprecipitated proteins showed that ATA strongly increased the amount of eNOS co-precipitated with PMCA4 (Fig 5A). No significant differences were observed in the amount of PMCA4 precipitated in control or ATA-treated cells (Fig 5A) ruling out an effect of ATA on the affinity of the immunoprecipitating antibody for

PMCA4. This result indicates that ATA promotes the association between PMCA4 and eNOS. Accordingly, functional experiments in HUVECs showed that ATA (250 nM) significantly attenuate NO synthesis in VEGF-stimulated cells (Fig 5B), excluding NO as an effector of the enhancement in angiogenesis mediated by ATA.

3.4. Low ATA levels are not toxic to endothelial cells

Our observations suggest that inhibition of PMCA4 with ATA has therapeutic potential for the promotion of blood vessel formation in situations characterized by insufficient angiogenesis. To evaluate this possibility we first monitored for any effect of ATA on endothelial cell viability. Exposure of HUVECs to 250 nM ATA did not affect proliferation or cell viability (Fig 6A), and also had no effect on the VEGF-induced phosphorylation (activation) status of Erk1/2 (Fig 6B), indicating that low ATA concentrations do not modify the activity of this proliferative signal transduction pathway.

In contrast, long-term exposure of HUVECs to a higher concentration (20 μM) reduced cell viability (Fig S3A) and abolished the ability of VEGF-stimulated HUVECs to form capillary-like structures in matrigel assays (Fig S3B). To investigate the reasons underlying the toxic effects of high concentrations of ATA on endothelial cells, we first determined whether micromolar concentrations of ATA might induce any changes in the pH of the culture medium. Analysis of cultures of HUVECs incubated in medium containing vehicle (DMSO), or ATA at low (0.25 μM) or high (20 μM) concentration for different periods showed no differences in the pH of the medium (Fig S3C). Another possibility to explain the harmful effect of 20 μM ATA on the viability of endothelial cells could be that high ATA concentrations in the culture medium might result in deleterious osmotic stress on the cells. To test this possibility we checked the activation of ATF-2, a transcription factor well-known to respond to osmotic stress [30, 31], in HUVECs grown in tissue culture medium containing low or high concentrations of ATA. No changes in the phosphorylation (activation) status of ATF-2 were detected in cells grown in medium containing 20 μM ATA compared to cells grown in 0.25 μM ATA or vehicle (DMSO) (Fig S3D). Osmotic stress induced by high concentration of NaCl in the medium resulted in ATF-2 phosphorylation confirming the suitably of the assay (Fig S3D).

To analyse potential toxic effects of ATA in a more physiological setting, we treated zebrafish embryos with increasing ATA concentrations. Consistent with the *in vitro* data, low ATA concentrations (50-100 μM) caused no significant damage to embryos, which developed a normal vascular anatomy (Fig S4). In contrast, exposure to ATA concentrations above 100 μM was associated with embryo death (Fig S4).

Although our results demonstrate proof-of-concept for pharmacological targeting of PMCA4 in therapeutic approaches, refined versions of ATA with high specificity for PMCA4 will be required to design efficient and safe clinical interventions.

3.5. ATA enhances post-ischaemic hindlimb perfusion in vivo

To evaluate *in vivo* the therapeutic potential of PMCA4 inhibition to promote reperfusion of ischaemic tissues, we used the mouse hindlimb ischaemia model. We have used two surgical approaches to induce different levels of ischaemia in the lower limb of mice [32, 33]. In a first approach, limb ischaemia was induced by proximal and distal ligation of a short fragment of the femoral artery with excision of the intervening segment. This procedure induces limb ischaemia by significantly reducing the flow of blood to the limb but still maintains a low degree of blood flow to the muscle. Initially we chose this model to maintain a low degree of blood flow that could mediate the delivery of ATA to the ischaemic organ. To evaluate the effect of ATA on this setting, vehicle (DMSO) or ATA was administered intraperitoneally 2 hours after surgery and daily for 3 more days. Given the harmful effects of high ATA concentrations (Fig S3 and S4) we selected a dose of 5 mg/Kg/day, which is not associated with damage in mice [34]. Laser Doppler imaging analysis of blood flow performed 4 days after surgery revealed a significant increase in the reperfusion of post-ischaemic limbs treated with ATA (Fig 7). To explore whether ATA would be able to exert the same effect in a model of deep acute ischaemia, in a separate set of experiments we performed femoral ligation and excision of the intervening segment but on this occasion we ligated and excised a longer femoral segment. This procedure totally blunted blood flow to the lower limb (Fig S5A). As expected, loss of blood flow resulted in a strong upregulation of VEGF expression in the ischaemic limb (Fig S6). Blood flow to the ischaemic limb was progressively recovered along time (Fig S5A). In

concurrence with our initial data, administration of ATA to these animals also enhanced significant reperfusion of the ischaemic limb (Fig S5A-B) although, in this case, administration of ATA for 7-10 days was required to detect the enhancement of blood flow mediated by the drug. It is likely that in this model, a longer period of ATA administration is required because ATA delivery to the ischaemic area is compromised during the first days post-surgery due to the absence of blood flow.

These data obtained using *in vivo* animal models reinforce the therapeutic potential of pharmacological targeting of PMCA4 to promote tissue reperfusion in patients with ischaemic cardiovascular disease.

4. Discussion

In this study, we demonstrate that inhibition of the plasma membrane calcium ATPase 4 (PMCA4) with low concentrations of the small polyaromatic compound aurintricarboxylic acid (ATA) significantly enhances VEGF-induced angiogenic processes. Our results show proof-of-concept for targeting PMCA4 therapeutically to improve VEGF-based pro-angiogenic interventions in patients with ischaemic cardiovascular disease. In this work we have used ATA to inhibit the function of PMCA4. The feasibility of ATA as a clinical treatment has yet to be tested, but pre-clinical studies in animal models have revealed potential clinical applications in the treatment of cardiac hypertrophy [34], experimental autoimmune encephalomyelitis [35], sepsis [36], and myocardial ischaemia-reperfusion injury [37].

Our results show that high levels of ATA strongly reduce endothelial cell viability and abolish tube formation. Consistent with our results, Lipo et al. [38] reported that increasing ATA concentrations diminish the ability of endothelial cells to form tubular-like structures in matrigel assays. Furthermore, in the same study, the authors report that intravitreal injection of 1.5 μg ATA in 2μl 10% DMSO (corresponding to 1.78 mM ATA) into mice strongly attenuates laser-induced choroidal neovascularization. It is highly likely that the reduced ocular vascularization observed by Lipo et al. [38] results from the toxicity associated with high ATA concentrations, an interpretation supported by our experiments in zebrafish embryos (Fig S4) and those reported by Smee et al. [39] in mice. Furthermore, 5-20 μM ATA has been shown to reduce the growth rate of fibroblasts [40] and smooth muscle cells [41]. In this work we have not identified the mechanisms underlying the harmful effect on endothelial cell viability exerted by high levels of ATA but, at these concentrations, ATA has been reported to non-specifically inhibit the action of nucleases [42], calpain [43] and several chemokine receptors [35], suggesting possible explanations for the toxicity of high-concentration ATA. The deleterious effects exerted by ATA at high concentrations indicate that refined, highly selective versions of this molecule will be required for efficient therapeutic interventions to treat patients with chronic ischaemic disease without associated harmful side-effects.

Mechanistically, ATA enhances VEGF-induced activation of the calcineurin/NFAT pathway in endothelial cells, in turn boosting calcineurin-dependent angiogenic processes such as endothelial cell migration and tubular morphogenesis. Our data indicate that ATA increases calcineurin signalling by disrupting its interaction with calcineurin at the plasma membrane. At present, we do not know the molecular process by which ATA disrupts the PMCA4/calcineurin complex. A possible explanation is masking by ATA of the calcineurin-interacting region in PMCA4 (amino acids 428 to 651 in human PMCA4b) [21]. Supporting this possibility, ATA inhibits hepatitis C helicase by a similar mechanism, binding to a defined region in the enzyme and thereby blocking interaction with nucleic acids [44]. However, a different picture emerges from analysis of the effect of ATA on PMCA4 binding to endothelial nitric oxide synthase (eNOS), which interacts with the same PMCA4 domain as calcineurin [26]. Rather than decreasing the interaction, ATA promotes association between PMCA4 and eNOS (Fig 5A). The opposite effects of ATA on PMCA4 binding to calcineurin or eNOS suggests that ATA is unlikely to be an allosteric competitor with partner proteins for binding to the 428-651 PMCA4 domain. It will be interesting in future research to fully define the molecular events implicated in ATA-mediated disruption of PMCA4/calcineurin interaction and the differential effect of ATA on PMCA4 binding to calcineurin or eNOS.

The results presented here establish a key role for the calcineurin/NFAT signalling pathway in the enhancement of VEGF-induced angiogenesis upon inhibition of PMCA4 with low ATA concentrations. We have previously reported that PMCA4 also downregulates eNOS activity and NO production in endothelial cells (26). Here, we show that ATA attenuates VEGF-induced nitric oxide production in endothelial cells, suggesting that NO signalling is not implicated in the enhancement of angiogenesis mediated by ATA; however, our results do not exclude the potential participation of other signalling pathways. Further investigations into the molecular mechanisms underlying ATA-mediated enhancement of VEGF signalling promise to reveal novel molecular targets for improving pro-angiogenic therapy.

Our *in vivo* experiments in animal models of experimentally induced hindlimb ischaemia show that ATA enhances reperfusion of post-ischaemic limbs. Given that our experiments using

HUVECs in culture have shown that ATA markedly enhances VEGF-induced angiogenesis *in vitro*, it is likely that the increase in reperfusion of post-ischaemic limbs induced by ATA involves increased revascularisation of the muscle, although a full characterisation of the effect of ATA on angiogenesis *in vivo* will require further investigations.

The present study indicates that targeting PMCA4 could improve VEGF-based pro-angiogenic interventions, highlighting the clinical potential of using PMCA4 inhibitors for the treatment of ischaemic cardiovascular disease. Interestingly, in addition to the ATA-mediated increase in reperfusion of ischaemic limbs, a trend to increase blood flow in non-ischaemic (sham-operated) muscle was also observed in the animals treated with ATA (Fig 7 and S5) although these differences did not reach statistical significance (P=0.0558). Our findings in cultured HUVECs have shown that ATA enhances blood vessel formation in the presence of VEGF but does not have any effect when it is added to serum-starved cells (Fig 4). We speculate that the increased blood flow in non-ischaemic limbs of animals treated with ATA might be the result of ATA acting in conjunction with low physiological levels of VEGF normally present in the muscle (Fig S6). We think this is extremely interesting from a therapeutic point of view, as one of the main obstacles for success of current VEGF-based therapeutic strategies is the difficulty to achieve high ectopic expression of VEGF in the ischaemic organ [5]. In fact, although it is thought that VEGF-based gene therapy is the best way forward in future therapeutic approaches, adenoviral vectors only transduce a small percentage of the target cells in humans [45]. Thus, selective PMCA4 inhibitors might be useful co-adjuvants in VEGF-based gene therapy strategies to enhance reperfusion of ischaemic tissues even in situations where expression of ectopic VEGF is not very high. Our *in* vivo data in this work do not allow evaluating the efficiency of single versus combined ATA/VEGF therapies. Further studies are required to analyse the pharmacokinetics of single and combined ATA/VEGF therapies in preclinical animal models of cardiovascular ischaemic disease.

Funding

This work was supported by the Research Institute in Healthcare Sciences, Faculty of Science and Engineering, University of Wolverhampton (to A.L.A.), and by an MRC programme grant (grant G1002082 to L.N. and E.J.C.). J.M.R. is supported by the Spanish Ministry of Economy and Competitiveness (MINECO) (grant SAF2015-636333R to J.M.R.) and CIBERCV of Ministerio de Sanidad (grant CB16/11/00264 to J.M.R.). S.K. and A.L.A. are supported by the Rosetrees Trust (grant M531 to A.L.A). S.M-M. and J.M.R. are supported by grants from the Fundacion La Marato TV3 (grant 20122532 to S.M-M. and grant 20151331 to J.M.R.). The Centro Nacional de Investigaciones Cardiovasculares (CNIC) is supported by the Spanish Ministry of Economy and Competitiveness (MINECO) and the Pro-CNIC Foundation, and is a Severo Ochoa Center of Excellence (MINECO award SEV-2015-0505).

Acknowledgments

We thank Simon Bartlett for English editing and Alicia Peral for technical assistance.

Conflict of Interest

None declared.

References

[1] Mozaffarian D, Benjamin EJ, Go AS, Arnett DK, Blaha MJ, Cushman M, de Ferranti S, Després JP, Fullerton HJ, Howard VJ, Huffman MD, Judd SE, Kissela BM, Lackland DT, Lichtman JH, Lisabeth LD, Liu S, Mackey RH, Matchar DB, McGuire DK, Mohler ER 3rd, Moy CS, Muntner P, Mussolino ME, Nasir K, Neumar RW, Nichol G, Palaniappan L, Pandey DK, Reeves MJ, Rodriguez CJ, Sorlie PD, Stein J, Towfighi A, Turan TN, Virani SS, Willey JZ, Woo D, Yeh RW, Turner MB, American Heart Association Statistics Committee and Stroke Statistics Subcommittee. Circulation 131(2015) e29-e322.

[2] Sachs T, Pomposelli F, Hamdan A, Wyers M, Schermerhorn M, Trends in the national outcomes and costs for claudication and limb threatening ischemia: angioplasty vs bypass graft, J. Vasc. Surg. 54 (2011) 1021-1031.

[3] Al Sabti H, Therapeutic angiogenesis in cardiovascular disease, J. Cardiothorac. Surg. 2 (2007) 49-55.

[4] Cooke JP, Losordo DW, Modulating the vascular response to limb ischemia: angiogenic and cell therapies, Circ. Res. 116 (2015) 1561-1578.

[5] Zachary I, Morgan RD, Therapeutic angiogenesis for cardiovascular disease: biological context, challenges, prospects, Heart 97 (2011) 181-189.

[6] Carmelit P, Jain RK, Molecular mechanisms and clinical applications of angiogenesis, Nature 473 (2011) 298-307.

[7] Takahashi H, Shibuya M, The vascular endothelial growth factor (VEGF)/VEGF receptor system and its role under physiological and pathological conditions, Clin. Sci. (Lond) 109 (2005) 227-241.

[8] Ylä-Herttuala S, Cardiovascular gene therapy with vascular endothelial growth factors, Gene 525 (2013) 217-219.

[9] Gupta R, Tongers J, Losordo DW, Human studies of angiogenic gene therapy, Circ. Res. 105 (2009) 724-736.

[10] Baggott RR, Alfranca A, López-Maderuelo D, Mohamed TM, Escolano A, Oller J, Ornes BC, Kurusamy S, Rowther FB, Brown JE, Oceandy D, Cartwright EJ, Wang W, Gómez-del Arco P, Martínez-Martínez S, Neyses L, Redondo JM, Armesilla AL, Plasma membrane calcium ATPase isoform 4 inhibits vascular endothelial growth factor-mediated angiogenesis through interaction with calcineurin, Arterioscler. Thromb. Vasc. Biol. 34 (2014) 2310-2320.

[11] Strehler EE, Caride AJ, Filoteo AG, Xiong Y, Penniston JT, Enyedi A, Plasma membrane Ca2+ ATPases as dynamic regulators of cellular calcium handling., Ann. Ny. Acad. Sci. 1099 (2007) 226-236.

[12] Pászty K, Caride AJ, Bajzer Ž, Offord CP, Padányi R, Hegedűs L, Varga K, Strehler EE, Enyedi A, Plasma membrane Ca^{2+}-ATPases can shape the pattern of Ca^{2+} transients induced by store-operated Ca^{2+} entry, Sci. Signal. 8 (2015) ra19.

[13] Klee CB, Ren H, Wang X, Regulation of the calmodulin-stimulated protein phosphatase, calcineurin. J. Biol. Chem. 273 (1998) 13367-13370.

[14] Hogan PG, Chen L, Nardone J, Rao A, Transcriptional regulation by calcium, calcineurin, and NFAT, Genes Dev. 17 (2003) 2205-2232.

[15] Armesilla AL, Lorenzo E, Gómez del Arco P, Martínez-Martínez S, Alfranca A, Redondo JM, Vascular endothelial growth factor activates nuclear factor of activated T cells in human endothelial cells: a role for tissue factor gene expression, Mol. Cell. Biol. 19 (1999) 2032-2043.

[16] Hernández GL, Volpert OV, Iñiguez MA, Lorenzo E, Martínez-Martínez S, Grau R, Fresno M, Redondo JM, Selective inhibition of vascular endothelial growth factor-mediated angiogenesis by cyclosporin A: roles of the nuclear factor of activated T cells and cyclooxygenase 2, J. Exp. Med. 193 (2001) 607-620.

[17] Mohamed TM, Abou-Leisa R, Baudoin F, Stafford N, Neyses L, Cartwright EJ, Oceandy D, Development and characterization of a novel fluorescent indicator protein PMCA4-GCaMP2 in cardiomyocytes, J. Mol. Cell. Cardiol. 63 (2013) 57-68.

[18] Schuh K, Cartwright EJ, Jankevics E, Bundschu K, Liebermann J, Williams JC, Armesilla AL, Emerson M, Oceandy D, Knobeloch KP, Neyses L, Plasma membrane Ca2+ ATPase 4 is required for sperm motility and male fertility, J. Biol. Chem. 279 (2004) 28220-28226.

[19] Holton M, Yang D, Wang W, Mohamed TM, Neyses L, Armesilla AL, The interaction between endogenous calcineurin and the plasma membrane calcium-dependent ATPase is isoform specific in breast cancer cells, FEBS Lett. 581 (2007) 4115-4119.

[20] Baggott RR, Mohamed TM, Oceandy D, Holton M, Blanc MC, Roux-Soro SC, Brown S, Brown JE, Cartwright EJ, Wang W, Neyses L, Armesilla AL Disruption of the interaction between PMCA2 and calcineurin triggers apoptosis and enhances paclitaxel-induced cytotoxicity in breast cancer cells, Carcinogenesis 33 (2012) 2362-2368.

[21] Buch MH, Pickard A, Rodriguez A, Gillies S, Maass AH, Emerson M, Cartwright EJ, Williams JC, Oceandy D, Redondo JM, Neyses L, Armesilla AL, The sarcolemmal calcium pump inhibits the calcineurin/nuclear factor of activated T-cell pathway via interaction with the calcineurin A catalytic subunit, J. Biol. Chem. 280 (2005) 29479-29487.

[22] Plumb JA, Milroy R, Kaye SB, Effects of the pH dependence of 3-(4,5-dimethylthiazol-2-yl)-2,5-diphenyl-tetrazolium bromide-formazan absorption on chemosensitivity determined by a novel tetrazolium-based assay, Cancer Res. 49 (1989) 4435-4440.

[23] Blum Y, Belting HG, Ellertsdottir E, Herwig L, Lüders F, Affolter M, Complex cell rearrangements during intersegmental vessel sprouting and vessel fusion in the zebrafish embryo, Dev. Biol. 316 (2008) 312-322.

[24] Hogan BM, Bos FL, Bussmann J, Witte M, Chi NC, Duckers HJ, Schulte-Merker S, Ccbe1 is required for embryonic lymphangiogenesis and venous sprouting, Nat. Genet. 41 (2009) 396-398.

[25] Holton ML, Wang W, Emerson M, Neyses L, Armesilla AL, Plasma membrane calcium ATPase proteins as novel regulators of signal transduction pathways, World J. Biol. Chem. 1 (2010) 201-208.

[26] Holton M, Mohamed TM, Oceandy D, Wang W, Lamas S, Emerson M, Neyses L, Armesilla AL, Endothelial nitric oxide synthase activity is inhibited by the plasma membrane calcium ATPase in human endothelial cells, Cardiovasc. Res. 87 (2010) 440-448.

[27] Luque Contreras D, Vargas Robles H, Romo E, Rios A, Escalante B, The role of nitric oxide in the post-ischemic revascularization process, Pharmacol. Ther. 112 (2006) 553-563.

[28] Ziche M, Morbidelli L, Nitric oxide and angiogenesis, J. Neurooncol. 50 (2000)139-148.

[29] Michell BJ, Griffiths JE, Mitchelhill KI, Rodriguez-Crespo I, Tiganis T, Bozinovski S, de Montellano PR, Kemp BE, Pearson RB, The Akt kinase signals directly to endothelial nitric oxide synthase, Curr. Biol. 9 (1999) 845-848.

[30] Wang L, Payton R, Dai W, Lu L, Hyperosmotic stress-induced ATF-2 activation through Polo-like kinase 3 in human corneal epithelial cells, J. Biol. Chem. 286 (2011) 1951-1958.

[31] Ouwens DM, de Ruiter ND, van der Zon GC, Carter AP, Schouten J, van der Burgt C, Kooistra K, Bos JL, Maassen JA, van Dam H, Growth factors can activate ATF2 via a two-step mechanism: phosphorylation of Thr71 through the Ras-MEK-ERK pathway and of Thr69 through RalGDS-Src-p38, EMBO J. 21 (2002) 3782-3793.

[32] Krishna SM, Omer SM, Golledge J, Evaluation of the clinical relevance and limitations of current pre-clinical models of peripheral artery disease, Clin. Sci. (Lond). 130 (2016) 127-150.

[33] Brenes RA, Jadlowiec CC, Bear M, Hashim P, Protack CD, Li X, Lv W, Collins MJ, Dardik A, Toward a mouse model of hind limb ischemia to test therapeutic angiogenesis, J Vasc Surg. 2012 Dec;56(6):1669-79

[34] Mohamed TM, Abou-Leisa R, Stafford N, Maqsood A, Zi M, Prehar S, Baudoin-Stanley F, Wang X, Neyses L, Cartwright EJ, Oceandy D, The plasma membrane

calcium ATPase 4 signalling in cardiac fibroblasts mediates cardiomyocyte hypertrophy, Nat. Commun. 7 (2016) 11074-11090.

[35] Zhang F, Wei W, Chai H, Xie X, Aurintricarboxylic acid ameliorates experimental autoimmune encephalomyelitis by blocking chemokine-mediated pathogenic cell migration and infiltration, J. Immunol. 190 (2013) 1017-1025.

[36] Laufenberg LJ, Kazi AA, Lang CH, Salutary effect of aurintricarboxylic acid on endotoxin- and sepsis-induced changes in muscle protein synthesis and inflammation, Shock 41 (2014) 420-428.

[37] Zhao ZQ, Morris CD, Budde JM, Wang NP, Muraki S, Sun HY, Guyton RA, Inhibition of myocardial apoptosis reduces infarct size and improves regional contractile dysfunction during reperfusion, Cardiovasc. Res. 59 (2003) 132-142.

[38] Lipo E, Cashman SM, Kumar-Singh R, Aurintricarboxylic acid inhibits complement activation, membrane attack complex, and choroidal neovascularization in a model of macular degeneration, Invest. Ophthalmol. Vis. Sci. 54 (2013) 7107-7114.

[39] Smee DF, Hurst BL, Wong MH, Lack of efficacy of aurintricarboxylic acid and ethacrynic acid against vaccinia virus respiratory infections in mice, Antivir. Chem. Chemother. 20 (2010) 201-205.

[40] Benezra M, Vlodavsky I, Yayon A, Bar-Shavit R, Regan J, Chang M, Ben-Sasson S, Reversal of basic fibroblast growth factor-mediated autocrine cell transformation by aromatic anionic compounds, Cancer Res. 52 (1992) 5656-5662.

[41] Benezra M, Ben-Sasson SA, Regan J, Chang M, Bar-Shavit R, Vlodavsky I, Antiproliferative activity to vascular smooth muscle cells and receptor binding of heparin-mimicking polyaromatic anionic compounds, Arterioscler. Thromb. Vasc. Biol. 14 (1994) 1992-1999.

[42] Hallick RB, Chelm BK, Gray PW, Orozco EM Jr, Use of aurintricarboxylic acid as an inhibitor of nucleases during nucleic acid isolation, Nucleic Acids Res 4 (1977) 3055-3064.

[43] Posner A, Raser KJ, Hajimohammadreza I, Yuen PW, Wang KK, Aurintricarboxylic acid is an inhibitor of mu- and m-calpain, Biochem. Mol. Biol. Int. 36 (1995) 291-299.

[44] Shadrick WR, Mukherjee S, Hanson AM, Sweeney NL, Frick DN, Aurintricarboxylic acid modulates the affinity of hepatitis C virus NS3 helicase for both nucleic acid and ATP, Biochemistry 52 (2013) 6151-6159.

[45] Ylä-Herttuala S, Alitalo K, Gene transfer as a tool to induce therapeutic vascular growth, Nat. Med. 9 (2003) 694-701.

Figure Legends

Figure 1. ATA enhances VEGF-induced activation of calcineurin/NFAT signalling in endothelial cells. (A) HUVECs infected with the NFAT-dependent luciferase reporter adenovirus AdNFAT-Luc (MOI=50) were treated with VEGF (25 ng/ml) or left untreated (control) in the presence of ATA (250 nM) or vehicle (DMSO). Cells were lysed 6 hours post stimulation and luciferase activity was determined as an index of calcineurin/NFAT pathway activity. Results are expressed as fold-induction over the calcineurin/NFAT activity in DMSO-treated control cells. Data are shown as mean ± SE, n=12, obtained from 3 independent experiments. ns=non-significant; ***, $P \leq 0.005$; $^{\#\#\#\#}$, $P \leq 0.001$; $^{\&\&\&\&}$, $P \leq 0.001$ (one-way ANOVA with *post hoc* Tukey´s comparison test). (B) HUVECs treated as in (A) were lysed 4 hours post stimulation, and protein lysates were analysed by western blot to determine the levels of RCAN1.4 and tubulin. RCAN1.4 levels were normalised to the amount of tubulin in each sample. Data are shown as mean ± SE, n=6, obtained from 3 independent experiments.*, $P \leq 0.05$ (unpaired two-tailed Student's *t* test) for comparison of cells treated with ATA *vs* vehicle (DMSO).

Figure 2. ATA releases calcineurin from interaction with PMCA4 in the endothelial cell plasma membrane. (A) Western blot analysis of calcineurin A (CnA), PMCA4, and cadherin in the plasma membrane protein fraction of serum-starved HUVECs treated for 4 hours with VEGF (25 ng/ml) plus ATA (250 nM) or vehicle (DMSO). The histogram shows the levels of membrane-associated calcineurin normalised to the amount of cadherin present in each sample. (B) Western blot analysis of calcineurin A (CnA), PMCA4 and tubulin (Tub) in total lysates prepared with Laemmli buffer from HUVECs treated as in (A). The histogram shows levels of total calcineurin normalised to the amount of tubulin present in each sample. (C) Immunoprecipitation/western blot analysis of calcineurin (CnA) and PMCA4 in protein complexes immunoprecipitated with anti-calcineurin antibody from total protein lysates of HUVECs treated as in (A). The histogram shows levels of co-precipitated PMCA4 normalised to the amount of calcineurin precipitated in each assay. (A-C) Blots are representative of 3 independent experiments. Histograms show data as mean ± SE, obtained from 3 independent experiments. **, $P \leq 0.01$ (unpaired two-tailed Student's *t* test) for comparison of the plasma membrane levels of calcineurin in VEGF-stimulated cells treated with ATA *vs* vehicle (DMSO). *, $P \leq 0.05$ (unpaired two-tailed Student's *t* test) for comparison of co-precipitated PMCA4 in VEGF-stimulated HUVECs treated with ATA *vs* vehicle (DMSO). ns=non-significant.

Figure 3 ATA increases endothelial cell motility by inhibiting PMCA4 and disrupting the PMCA4/calcineurin interaction. Representative images of wound-healing migration assays performed with HUVECs (A), $PMCA4^{+/+}$ or $PMCA4^{-/-}$ MLECs (B), and AdLacZ- or AdID4-infected HUVECs (C) incubated in culture medium supplemented with VEGF (25 ng/ml) in the presence of ATA (250 nM) or vehicle (DMSO). (A) Data are shown as mean ± SE, n=9, obtained from 3 independent experiments. ***, $P \leq 0.005$ (unpaired two-tailed, Student's *t* test) for comparison of cells treated with ATA *vs* vehicle (DMSO). (B) Data are shown as mean ± SE, n=6, obtained from 3 independent experiments. Differences were analysed for statistical significance by one-way ANOVA with *post hoc* Tukey´s comparison test. ***, $P \leq 0.005$ for comparison of migration by $PMCA4^{+/+}$ MLECs treated with ATA *vs* vehicle (DMSO). $^{\#\#\#\#}$, $P \leq 0.001$ for comparison of motility in wild-type (+/+) *vs* PMCA4 knockout (-/-) MLECs. ns=non-significant. (C) Data are shown as mean ± SE, n=3, obtained from 3 independent experiments. Differences were analysed for statistical significance by one-way ANOVA with *post hoc* Tukey´s comparison test. *, $P \leq 0.05$ for comparison of motility in AdLacZ-infected cells treated

with ATA *vs* vehicle (DMSO). ###, *P*≤0.005 for comparison of migration in cells infected with AdLacZ *vs* AdID4. ns=non-significant. Images in (A-C) were taken at time zero and after incubation for 24 hours. The migrated area was calculated by subtracting the value of the non-migrated area from the wound area at time zero, and expressing this as a percentage of the total area at time zero. Scale bars, 1000 µm.

Figure 4 ATA enhances endothelial cell tubular morphogenesis induced by VEGF but not by bFGF. HUVECs plated on Growth-Factor Reduced Matrix (Geltrex) in Medium 200 containing 2% FBS, were treated when indicated with VEGF (50 ng/ml) (A) or bFGF (50 ng/ml) (C) in the presence of ATA (250 nM) or vehicle (DMSO). Images show representative fields from experiments quantified in the histogram. Data are shown as mean ± SE, n=6 in (A) and n=4 in (C), and were obtained from 3 and 2 independent experiments, respectively. (A) ns=non-significant; ***, *P*≤0.005; #, *P*≤0.05; ####, *P*≤0.001; &, *P*≤0.05; &&&&, *P*≤0.001 (unpaired two-tailed Student's *t* test). (C) ns=non-significant; **, *P*≤0.01; ***, *P*≤0.005; ### , *P*≤0.005 (one-way ANOVA with *post hoc* Tukey's comparison test). (B) Tubular morphogenesis analysis in HUVECs transfected with a PMCA4-specific siRNA (si-PMCA4) or a non-targeting control siRNA (si-NT). Transfected cells were plated on Growth-Factor Reduced Matrix (Geltrex) in Medium 200 containing 2% FBS, and treated with VEGF (50 ng/ml) in the presence of ATA (250 nM) or vehicle (DMSO). Images show representative fields from experiments quantified in the histogram. Data are shown as mean ± SE, n=9 obtained from 3 independent experiments. ns=non-significant; ***, *P*≤0.005 (one-way ANOVA with *post hoc* Tukey's comparison test). (A-C) Scale bars, 1000 µm.

Figure 5 ATA treatment potentiates the PMCA4/eNOS interaction and attenuates nitric oxide synthesis in endothelial cells stimulated with VEGF. (A) Serum-starved HUVECs were treated with VEGF (25 ng/ml) and ATA (250 nM) or vehicle (DMSO) for 5 minutes. Protein lysates were immunoprecipitated with the anti-PMCA 5F10 monoclonal antibody, and levels of PMCA4 and eNOS in the immunoprecipitated proteins analysed by western blot. Histogram shows levels of co-precipitated eNOS normalised to the amount of PMCA4 precipitated in each assay. Data are shown as mean ± SE obtained from 3 independent experiments. ** indicates statistically significant differences (*P*≤0.01, according to unpaired, two-tailed Student's *t* test) in the levels of eNOS co-precipitated in samples treated with ATA vs DMSO. Western blot images are representative of 3 independent immunoprecipitation experiments. (B) HUVECs were treated as indicated in (A). Intracellular levels of nitric oxide were determined by staining cells with the NO-sensitive dye DAF-FM. Images showing microscopy fields of DAF-FM staining in cells are representative of 2 independent experiments. Scale bars, 20 µm.

Figure 6 Low concentration ATA is not toxic to endothelial cells. (A) MTT assay cell viability in HUVECs after overnight incubation (t=0) and incubation for 3 and 6 days in medium supplemented with VEGF (25 ng/ml) in the presence of ATA (250 nM) or vehicle (DMSO). Data are shown as mean ± SE, n=3, obtained from 3 independent experiments. (B) Western blot analysis of the phosphorylation (activation) status of Erk1-2 proteins in HUVECs stimulated as indicated with VEGF for 5 minutes in the presence of ATA (250 nM) or vehicle (DMSO). Data are shown as mean ± SE, n=5, obtained from 3 independent experiments. Erk1-2 phosphorylation levels were normalized to the amount of total Erk1-2 present in each sample. Data are expressed as the fold-induction in Erk1-2 phosphorylation relative to the value in unstimulated cells. ns=non-significant.

Figure 7 Administration of ATA at low concentration boosts post-ischaemic hind limb perfusion in mice. Representative laser Doppler images showing blood flow at 4 days after surgery in sham-operated non-ischaemic legs (S) and femoral-ligated ischaemic legs (I) of mice receiving ATA (5 mg/kg/day) or vehicle (DMSO) by intraperitoneal injection. Data are shown as mean ± SE, n=7, obtained from 2 independent experiments. **, $P \leq 0.01$ (unpaired two-tailed Student's *t* test) for comparison of ischaemic-leg blood flow in mice receiving ATA *vs* vehicle. ns=non-significant.

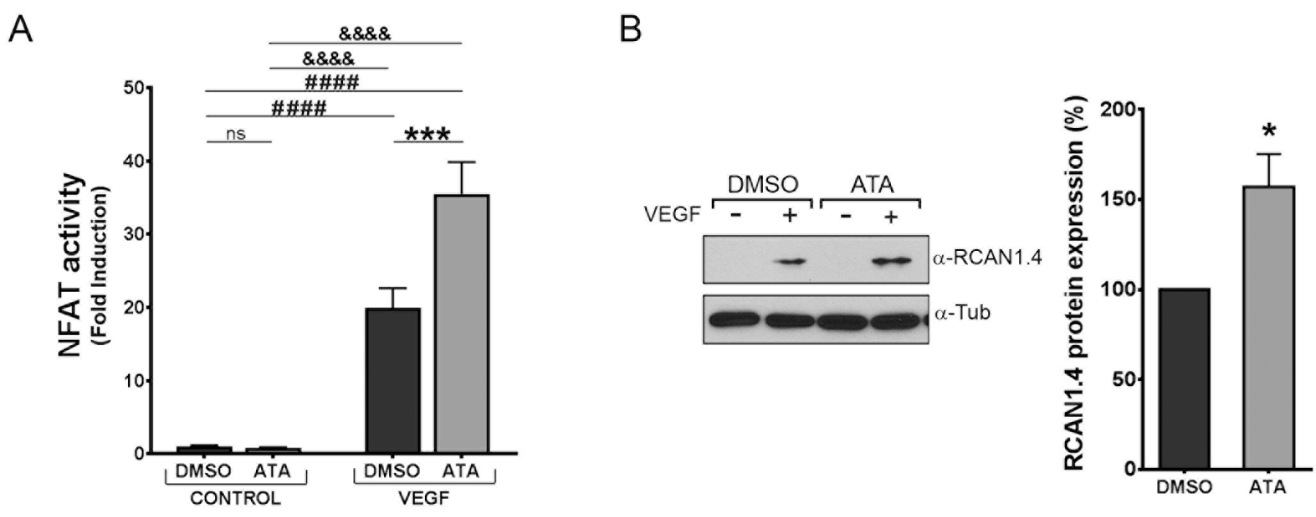
A
&&&&
&&&&
####
####
ns
***
NFAT activity
(Fold Induction)
50
40
30
20
10
0
DMSO
ATA
DMSO
ATA
CONTROL
VEGF
B
DMSO
ATA
VEGF
-
+
-
+
α-RCAN1.4
α-Tub
RCAN1.4 protein expression (%)
200
150
100
50
0
*
DMSO
ATA

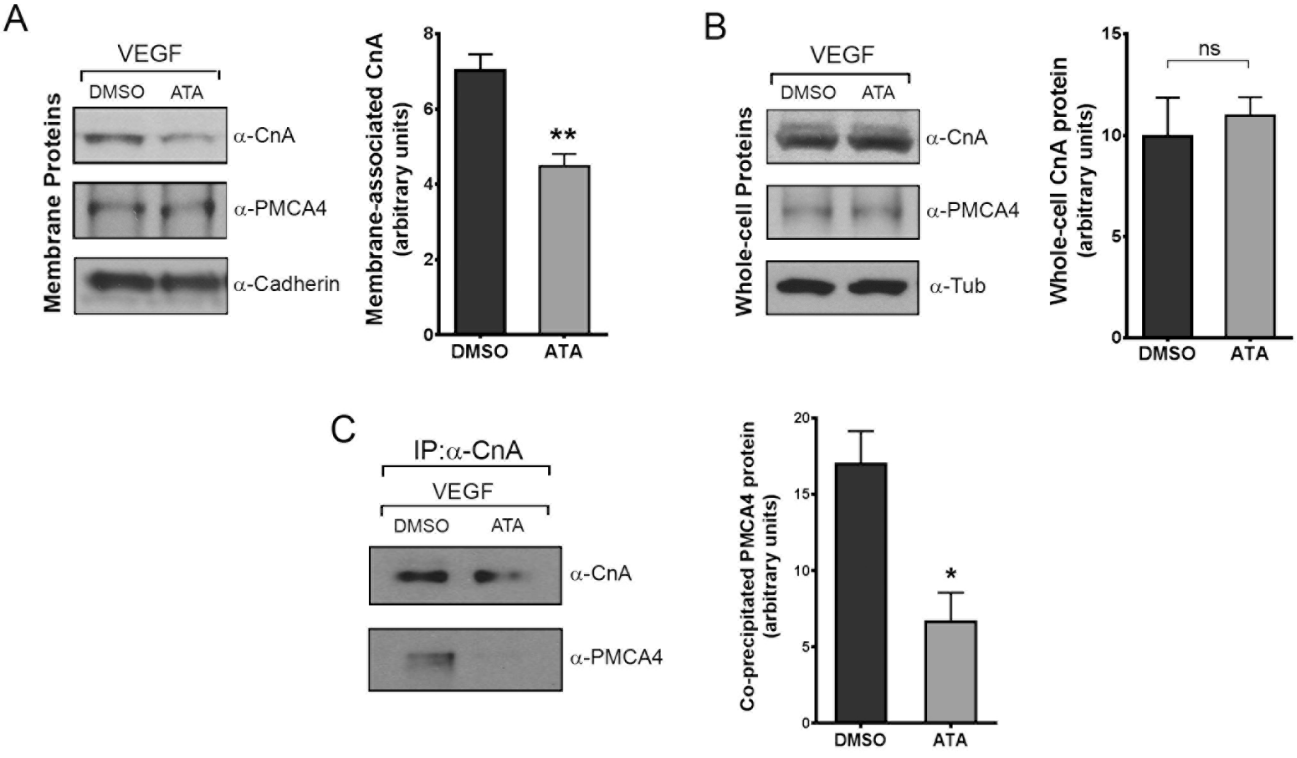
A
VEGF
DMSO
ATA
Membrane Proteins
α-CnA
α-PMCA4
α-Cadherin
Membrane-associated CnA (arbitrary units)
**
DMSO
ATA
B
VEGF
DMSO
ATA
Whole-cell Proteins
α-CnA
α-PMCA4
α-Tub
Whole-cell CnA protein (arbitrary units)
ns
DMSO
ATA
C
IP:α-CnA
VEGF
DMSO
ATA
α-CnA
α-PMCA4
Co-precipitated PMCA4 protein (arbitrary units)
*
DMSO
ATA

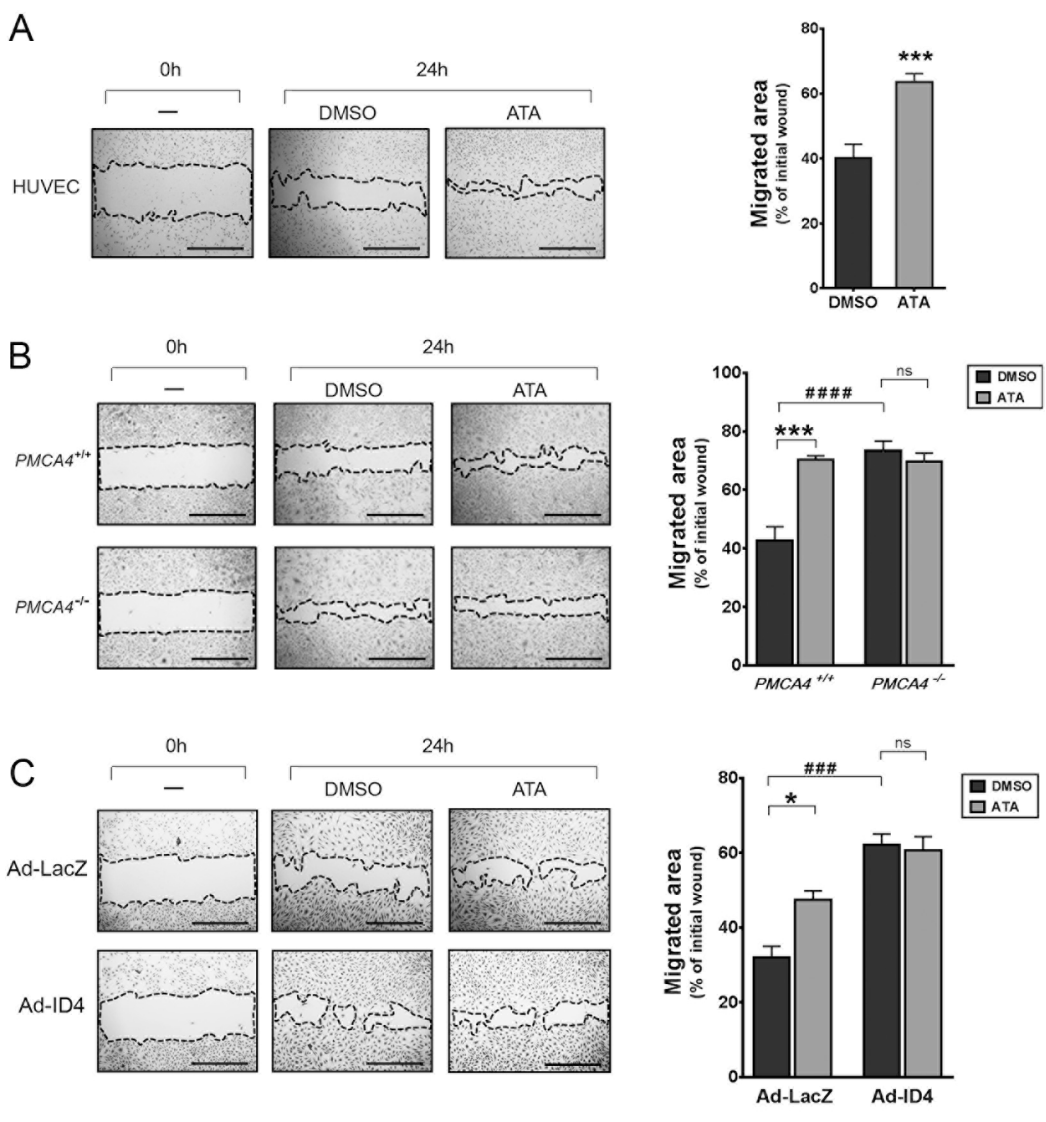
A
0h
24h
—
DMSO
ATA
HUVEC
Migrated area
(% of initial wound)
***
DMSO
ATA
B
0h
24h
—
DMSO
ATA
PMCA4+/+
PMCA4-/-
Migrated area
(% of initial wound)
####
ns
***
DMSO
ATA
PMCA4 +/+
PMCA4 -/-
C
0h
24h
—
DMSO
ATA
Ad-LacZ
Ad-ID4
Migrated area
(% of initial wound)
###
ns
*
DMSO
ATA
Ad-LacZ
Ad-ID4

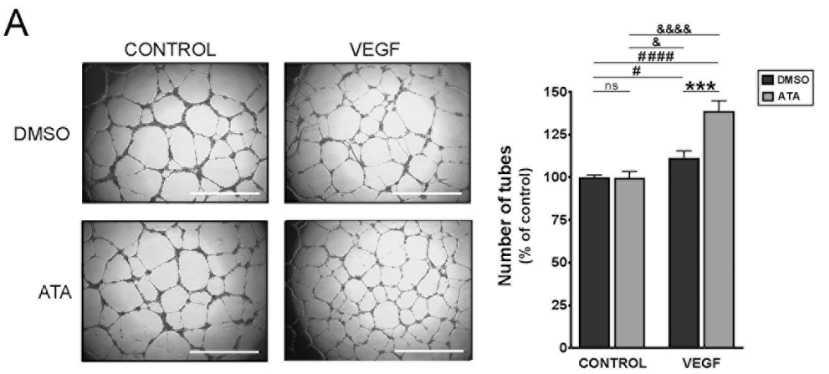
A
CONTROL
VEGF
DMSO
ATA
&&&&
&
####
#
ns
***
DMSO
ATA
Number of tubes
(% of control)
150
125
100
75
50
25
0
CONTROL
VEGF

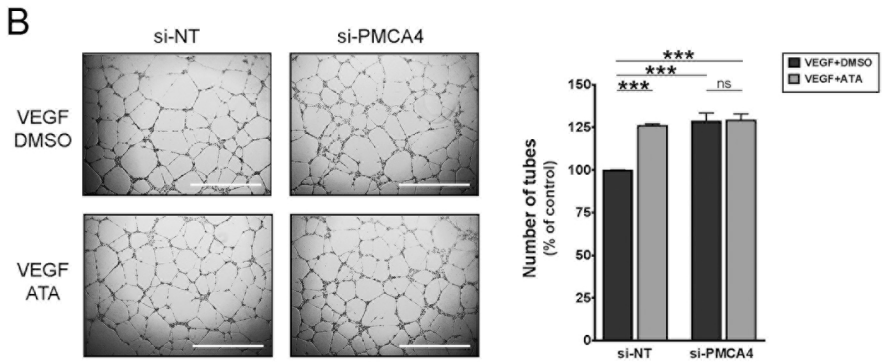
B
si-NT
si-PMCA4
VEGF
DMSO
VEGF
ATA
***
***
***
ns
VEGF+DMSO
VEGF+ATA
Number of tubes
(% of control)
150
125
100
75
50
25
0
si-NT
si-PMCA4

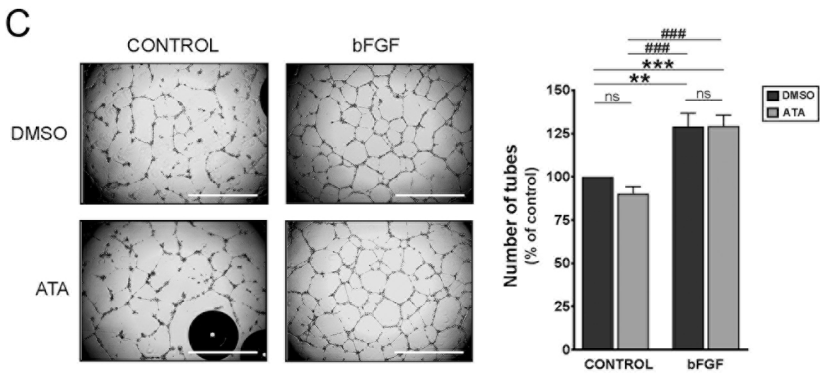
C
CONTROL
bFGF
DMSO
ATA
###
###
***
**
ns
ns
DMSO
ATA
Number of tubes
(% of control)
150
125
100
75
50
25
0
CONTROL
bFGF

A

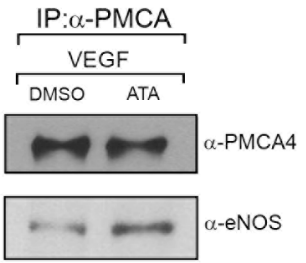
IP:α-PMCA
VEGF
DMSO
ATA
α-PMCA4
α-eNOS

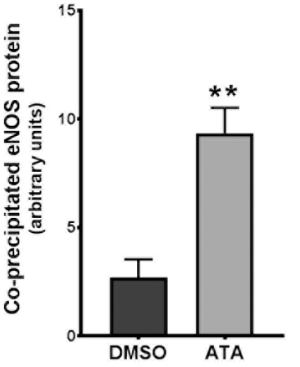
Co-precipitated eNOS protein
(arbitrary units)
15
10
5
0
**
DMSO
ATA

B

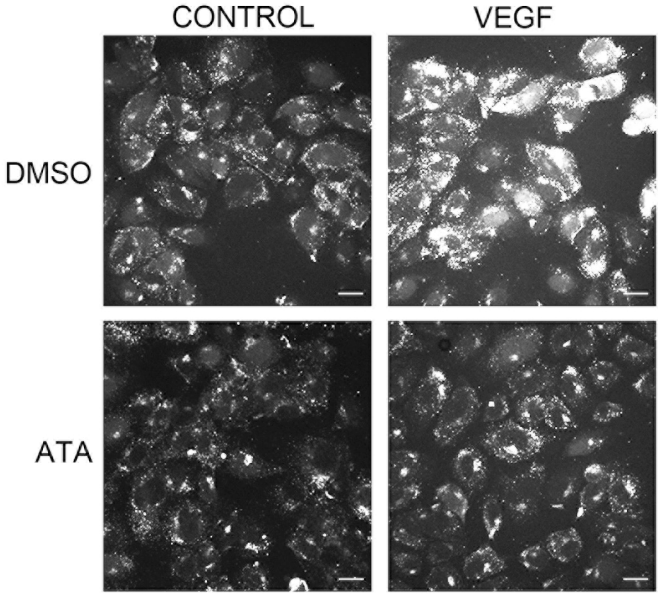
CONTROL
VEGF
DMSO
ATA

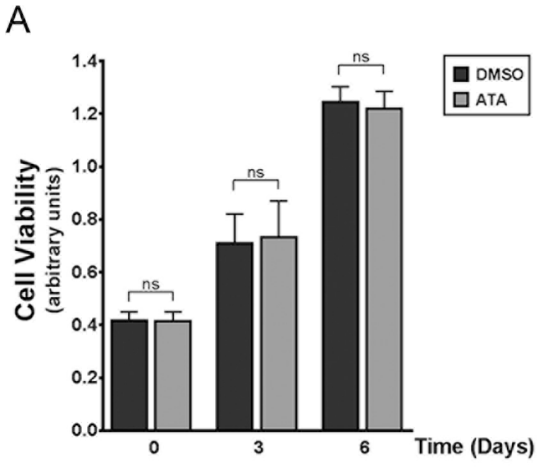
A
Cell Viability
(arbitrary units)
1.4
1.2
1.0
0.8
0.6
0.4
0.2
0.0
ns
ns
ns
DMSO
ATA
0
3
6
Time (Days)

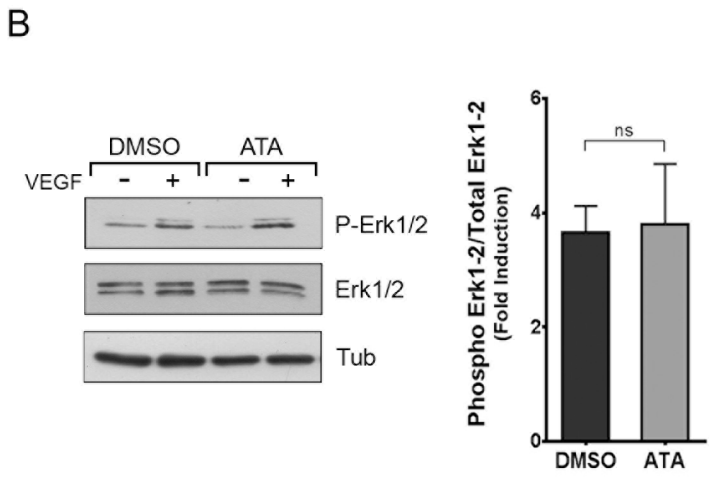
B
DMSO
ATA
VEGF
-
+
-
+
P-Erk1/2
Erk1/2
Tub
Phospho Erk1-2/Total Erk1-2
(Fold Induction)
6
4
2
0
ns
DMSO
ATA

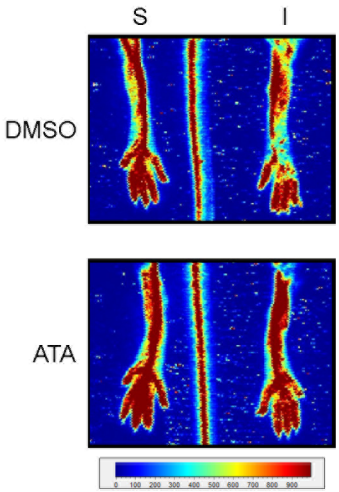
S
I
DMSO
ATA
0 100 200 300 400 500 600 700 800 900

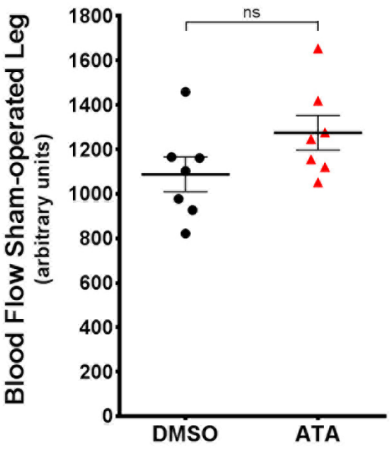
Blood Flow Sham-operated Leg
(arbitrary units)
ns
1800
1600
1400
1200
1000
800
600
400
200
0
DMSO
ATA

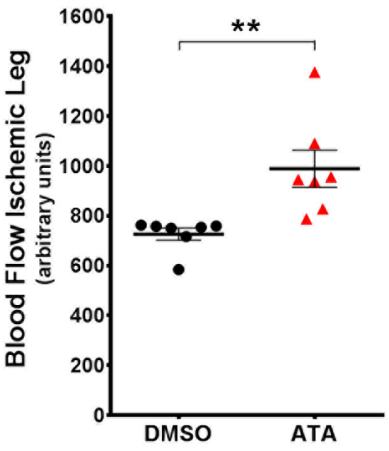
Blood Flow Ischemic Leg
(arbitrary units)
**
1600
1400
1200
1000
800
600
400
200
0
DMSO
ATA

ON LINE SUPPLEMENTARY DATA

Selective Inhibition of Plasma Membrane Calcium ATPase 4 improves angiogenesis and vascular reperfusion

Sathishkumar Kurusamy, Dolores López-Maderuelo, Robert Little, David Cadagan, Aaron M Savage, Jude C Ihugba, Rhiannon R Baggott, Farjana B Rowther, Sara Martínez-Martínez, Pablo Gómez-del Arco, Clare Murcott, Weiguang Wang, J Francisco Nistal, Delvac Oceandy, Ludwig Neyses, Robert N Wilkinson, Elizabeth J Cartwright, Juan Miguel Redondo, Angel Luis Armesilla

Supplementary Materials

Western blot antibodies

Western blot membranes were incubated in TBS-T (TBS, 0.05% Tween 20), overnight, at 4°C with a solution containing one of the following antibodies; for detection of RCAN1.4 with a 1:1000 dilution of a rabbit anti-DSCR1 polyclonal antibody (Sigma), for PMCA4 detection with a 1:500 dilution of the anti-PMCA4-specific monoclonal antibody JA3 (Santa Cruz Biotechnology), for detection of calcineurin with a 1:1000 dilution of a anti-calcineurin A monoclonal antibody (BD Biosciences), for detection of eNOS with a 1:5000 solution of a rabbit polyclonal anti-eNOS (Sigma), for detection of tubulin with a 1:2500 dilution of a mouse monoclonal anti-tubulin antibody (Sigma), for detection of total Erk with a 1:1000 dilution of a rabbit anti-Erk1/2 antibody (Cell Signalling), for detection of phosphorylated (activated) Erk1/2 with a 1:000 dilution of anti-phospho-Erk1/2 (Thr202/Tyr204) antibody (Cell Signalling), for detection of total ATF-2 with a 1:1000 dilution of a rabbit anti-ATF-2 antibody (Cell Signalling), for detection of phosphorylated (activated) ATF-2 with a 1:1000 dilution of anti-phospho-ATF-2 (Thr71) antibody (Cell Signalling).

After incubation with primary antibodies, membranes were washed with TBS-T, and then incubated in either a 1:5000 dilution of peroxidase-conjugated sheep anti-mouse immunoglobuilin antibody (Sigma) or 1:5000 dilution of peroxidase-conjugated donkey anti-

rabbit immunoglobulin antibody (GE Healthcare) depending of the origin of the primary antibody. Bound antibodies were detected by ECL.

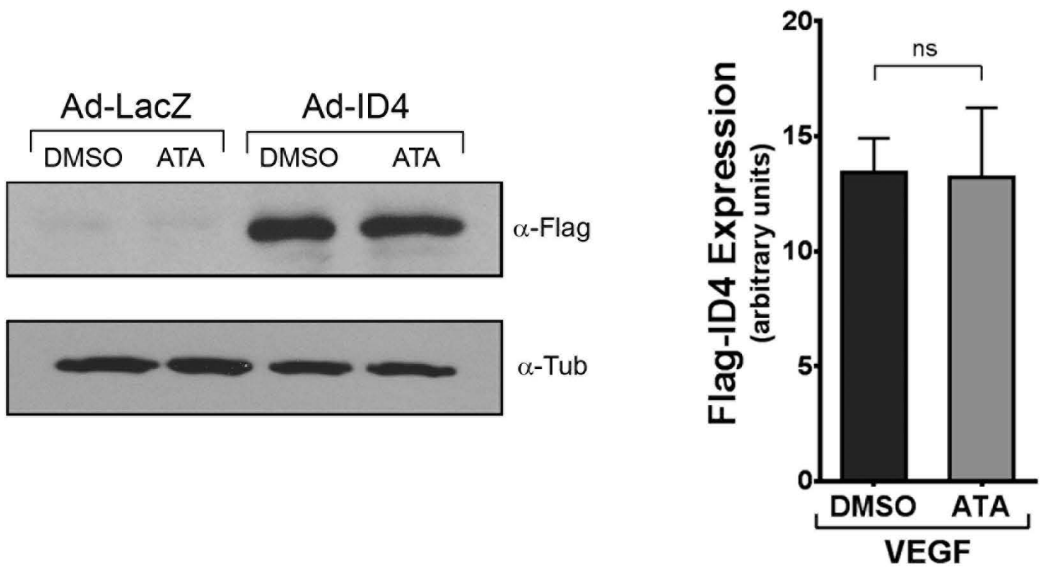

Figure S1. ATA does not alter the adenovirus-mediated expression of Flag-ID4. HUVECs infected (MOI=150) with Ad-LacZ (encoding β-galactosidase) or Ad-ID4 (encoding a Flag-tagged version of the domain of PMCA4 implicated in the interaction with calcineurin) were incubated in culture medium supplemented with VEGF (25 ng/ml) in the presence of ATA (250 nM) or vehicle (DMSO). Infected cells were lysed and the expression of Flag-ID4 analysed by western blot using the anti-Flag M2 monoclonal antibody. Expression levels of Tubulin (Tub) were analysed in the same samples as loading control. Histogram shows data as mean ± SE, n=3, obtained from 3 independent experiments. Data were analysed for statistically significant differences by unpaired two-tailed Student *t* test. ns=non-significant.

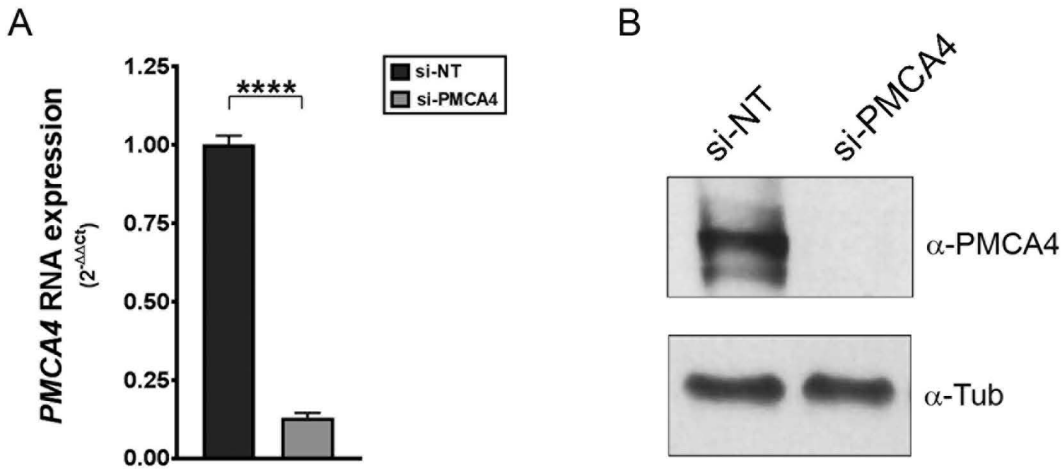

Figure S2. Small interfering RNA (siRNA) mediated knockdown of PMCA4 expression in endothelial cells. (A) *PMCA4* RNA levels in HUVECs transfected with a non-targeting control siRNA (si-NT) or a siRNA specific for human PMCA4 (si-PMCA4) were determined by qRT-PCR. Histograms show data as mean ± SE, n=9, obtained from 3 independent experiments. Data were analysed for statistically significant differences by unpaired two-tailed Student *t* test. **** indicates statistically significant differences ($P \leq 0.001$). (B) Analysis of PMCA4 protein expression in HUVECs transfected as in (A) using the anti-PMCA4 specific JA3 monoclonal antibody (α-PMCA4) or an anti-tubulin (α-Tub) antibody as a loading control. Western blot images are representative of 3 independent experiments.

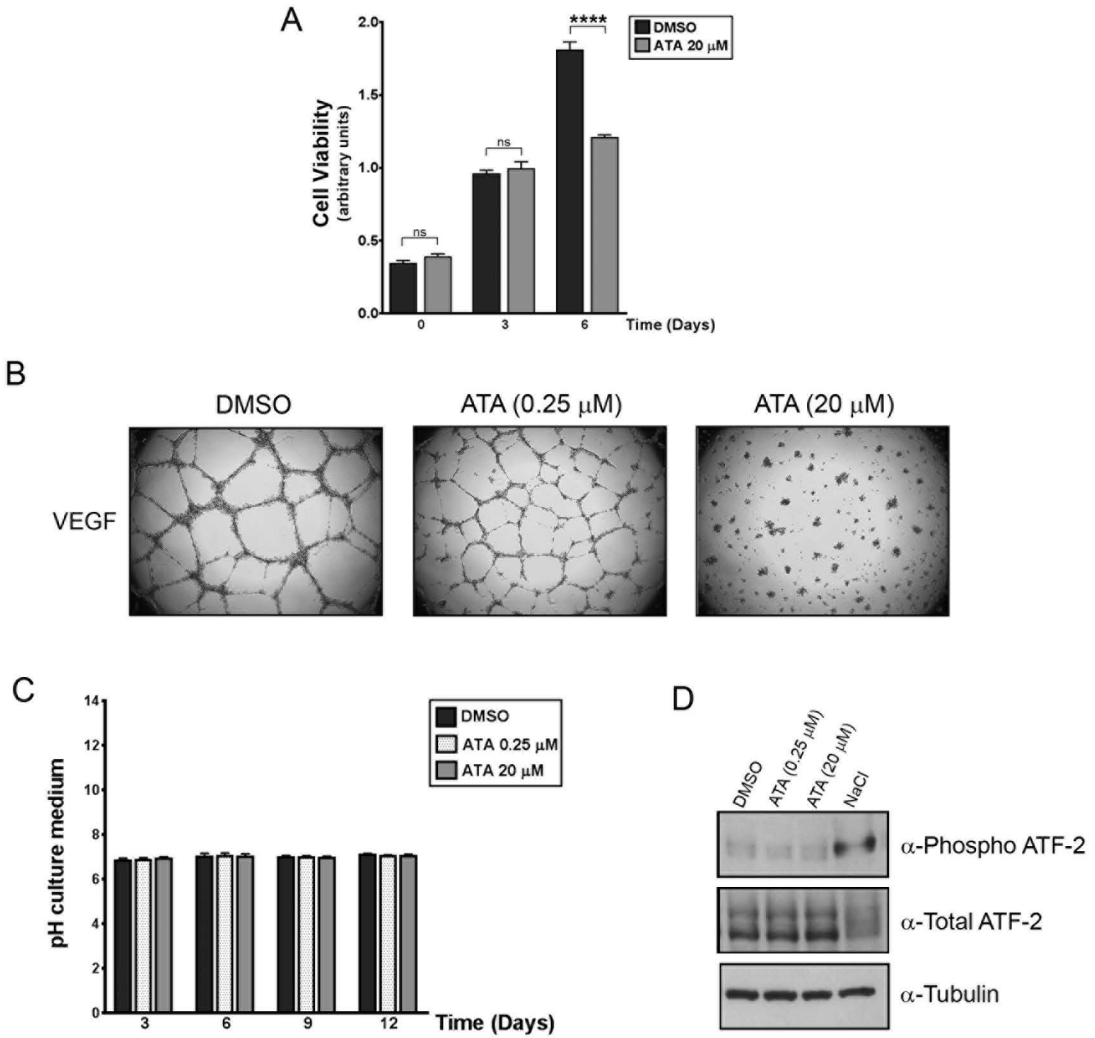

Figure S3. HUVECs exposure to 20 μM ATA reduces cell viability and impairs tube formation. (A) HUVECs were cultured in endothelial cell medium in the presence of 20 μM ATA or vehicle (DMSO) for 1 week changing medium every 2-3 days. Subsequently, cells were plated on 96-well plates and viability determined by MTT assay after overnight incubation (t=0) and after incubation for 3 and 6 days in culture medium supplemented with VEGF (25 ng/ml) in the presence of 20 μM ATA or DMSO. Histogram shows data as mean ± SE, n=4, obtained from 4 independent experiments. Results were analysed for statistically significant differences by one-way ANOVA with post hoc Tukey's comparison test. ****indicates statistically significant differences ($P \leq 0.001$) when comparing cells incubated in the presence of 20 μM ATA vs DMSO. ns=non-significant. (B) HUVECs were incubated in endothelial cell medium in the presence of 0.25 μM ATA, 20 μM ATA or DMSO for 1 week changing medium every 2-3 days. Cells were detached and re-plated on a layer of Growth-Factor Reduced Matrix (Geltrex) in Medium 200 containing 2% fetal bovine serum and VEGF (50 ng/ml) in the presence of 0.25 μM ATA, 20 μM ATA or DMSO and incubated for 24 hours longer. Images show representative results of two independent experiments. (C) HUVECs were incubated in endothelial cell medium in the presence of 0.25 μM ATA, 20 μM ATA or DMSO for 12 days changing medium every 3 days, and including VEGF (25 ng/ml) after 6 days to reproduce the conditions used in (A). pH of the medium was determined at the indicated times. Histogram shows data as mean ± SE, n=6, obtained from 3 independent experiments. Analyses of data by one-way ANOVA with post hoc Tukey's comparison test did not show statistically significant differences. (D) Incubation with high concentrations of ATA does not induce osmotic stress in endothelial cells.HUVECs were incubated in endothelial cell medium in the presence of 0.25 μM ATA, 20 μM ATA, NaCl 300 mM or DMSO for 20 minutes, and phosphorylation (activation) of the transcription factor ATF-2 was determined by western blot using an anti-phospho ATF-2 specific antibody as a surrogate measure of osmotic cellular stress. Levels of total ATF-2 and tubulin were also determined to establish protein loading in each sample. Images are representative of two independent experiments.

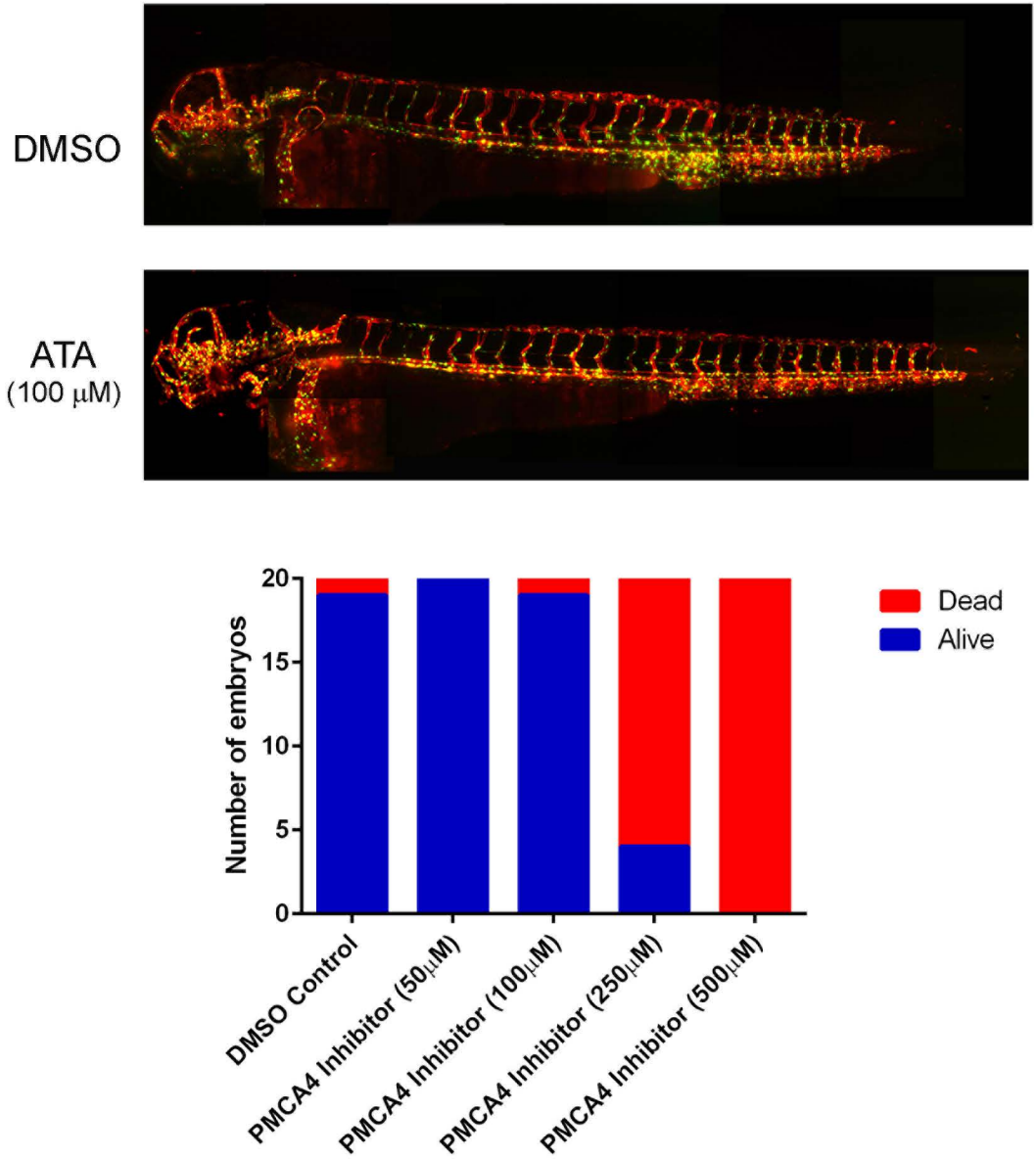

Figure S4. ATA treatment is toxic to zebrafish embryos at concentrations over 100 μM. Zebrafish *Tg(kdrl:HRAS-mCherry; flk1:EGFP-nls)* dechorionated embryos were incubated for 24 hours with increasing concentrations of the selective PMCA4 inhibitor ATA or vehicle (DMS0) from 30 hours post fertilisation (hpf). Vascular morphology was imaged at 54 hpf using a Zeiss Lightsheet Z.1 microscope. Images show vascular morphology in embryos treated with 100 μM ATA or DMSO. Membrane-tagged endothelial mCherry (red). Endothelial cell nuclei (green). Histogram shows embryo viability 24 hours after treatment. Results are representative of 2 independent experiments.

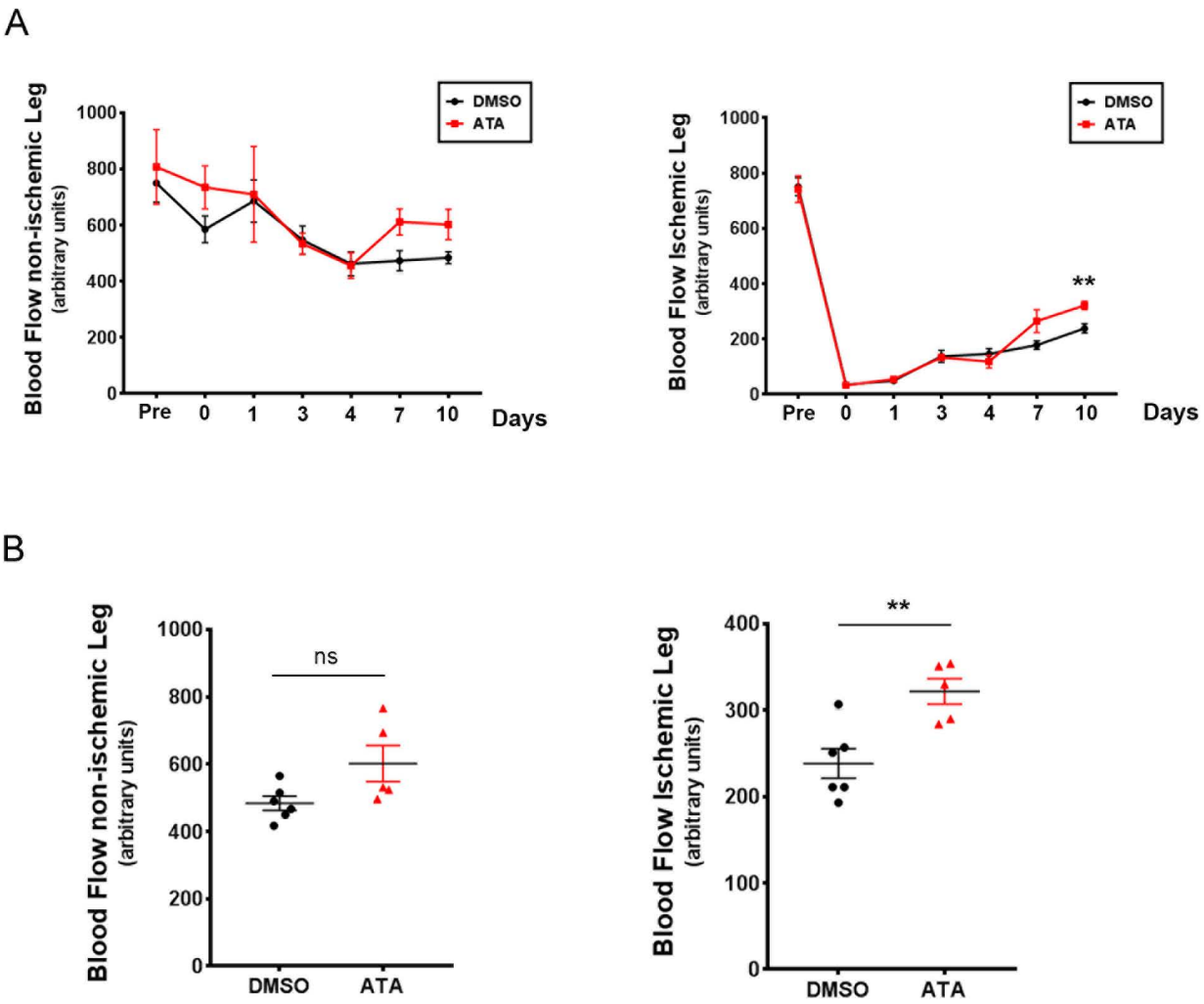

Figure S5. ATA enhances post-ischaemic limb reperfusion after deep acute ischaemia. Unilateral deep acute hind limb ischaemia was induced in mice by proximal and distal ligation of a long fragment of the femoral artery with excision of the intervening segment. (A) Time course analysis of blood flow by laser Doppler in sham-operated (non-ischaemic) or ischaemic limbs of mice receiving ATA (5 mg/kg/day) or vehicle (DMSO) by daily intraperitoneal injection for the indicated times. Blood flow was measured prior to operation (Pre), 2 hours after operation (0), and at the indicated times. **, $P \leq 0.01$(unpaired two-tailed Student's *t* test). (B) Scatter plot analysis of blood flow in the limbs of mice described in (A) at 10 days post-operation. **, $P \leq 0.01$(unpaired two-tailed Student's *t* test). n=6 for the group treated with vehicle (DMSO) and n=5 for the group treated with ATA.

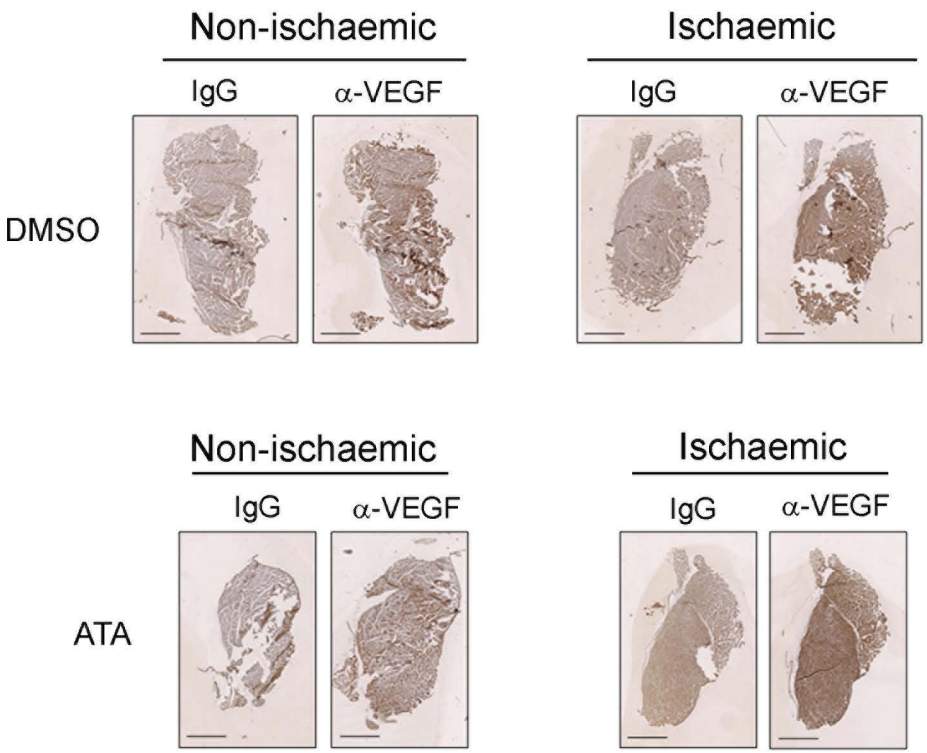

Figure S6. Experimentally-induced murine hind limb ischaemia is accompanied by upregulation of VEGF expression. Immunohistochemistry staining of VEGF in histological sections of non-ischaemic (sham-operated) or ischaemic tibialis muscle isolated from mice treated with vehicle (DMSO) or ATA (5 mg/kg/day) for 10 days. A rabbit anti-VEGF (α-VEGF) polyclonal antibody (1.4 μg/ml, final concentration) was used to detect VEGFexpression. Staining using rabbit IgG (IgG) at the same concentration was used as negative control. Scale bars, 1 mm.